A Comparison of Sentinel-1 Biased and Unbiased Coherence for Crop Monitoring and Classification

Qinxin Zhao [1], Qinghua Xie [1, *], Xing Peng [1], Yusong Bao [1], Tonglu Jia [1], Linwei Yue [1], Haiqiang Fu[2], Jianjun Zhu[2]

[1] The School of Geography and Information Engineering, China University of Geosciences (Wuhan), Wuhan 430074, China - (qinxinzhao, xieqh, pengxing, yusongbao, jtlcug, yuelw) @ cug.edu.cn
[2] The School of Geosciences and Info-Physics, Central South University, Changsha 410083, China - (haiqiangfu, zjj) @csu.edu.cn

Keywords: SAR, Coherence, Crop monitoring, Crop classification, Sentinel-1, Agriculture.

Abstract

Synthetic Aperture Radar (SAR) holds significant potential for applications in crop monitoring and classification. Interferometric SAR (InSAR) coherence proves effective in monitoring crop growth. Currently, the coherence based on the maximum likelihood estimator is biased towards low coherence values. Therefore, the main aim of this work is to access the performance of Sentinel-1 time-series biased coherence and unbiased coherence in crop monitoring and classification. This study was conducted during the 2018 growing season (April-October) in Komoka, an agricultural region in southwestern Ontario, Canada, primarily cultivating three crops: soybean, corn, and winter wheat. To verify the ability of coherence to monitor crops, a linear correlation coefficient between temporal coherence and dual polarimetric radar vegetation index (DpRVI) was fitted. The results revealed a stable correlation between temporal coherence and DpRVI time-series, with the highest correlation observed for soybean ($0.7 < R < 0.8$), followed by wheat and corn. Notably, unbiased coherence of the VV channel exhibited the highest correlation ($R > 0.75$). In addition, we applied unbiased coherence to crop classification. The results show that unbiased coherence exhibits very promising classification performance, with the overall accuracy (84.83%) and kappa coefficient (0.76) of VV improved by 8.35% and 0.12, respectively, over biased coherence, and the overall accuracy (73.25%) and kappa coefficient (0.57) of VH improved by 7.56% and 0.14, respectively, over biased coherence, and all crop classification accuracies were also effectively improved. This study demonstrates the feasibility of coherence monitoring of crops and provides new insights in enhancing the higher separability of crops.

1. Introduction

Synthetic Aperture Radar (SAR) technology, operating under all day and all-weather conditions, acquires vegetation information from the ground using longer wavelength microwave signals. With its excellent penetration of the vegetation canopy and high sensitivity to crop structure, SAR greatly contributes to crop monitoring and classification (Mandal et al., 2019). In this regard, the freely accessible C-band Sentinel-1 imagery provides high-quality Earth observation data globally on a 12-day revisit cycle (6 days within Europe), which is part of the Copernicus program. Dual-polarization SAR sensors have both polarization and interferometric features that allow the monitoring of crop growth changes in time-series, significantly promoting more relevant researches in agriculture (Bhogapurapu et al., 2021).

The backscattering coefficient of polarimetric SAR directly reflects crop characteristics based on the different interactions between microwave signals and crops. This confers a certain advantage upon the backscattering coefficient and its derived features in crop monitoring and classification, including radar vegetation indices and polarization decomposition suitable for various scenarios. However, crop growth is dynamic, influenced by factors such as growth morphology, environmental conditions, and agricultural practices. To comprehensively capture the scattering mechanisms of crops at various phenological stages, interferometric SAR (InSAR) coherence quantifies the correlation between of the scattering mechanisms of vegetation attributes during two SAR imaging periods (Rosen et al., 2002), thereby providing valuable temporal insights for crop. The

Sentinel-1 coherence obtained through revisit cycles of 6 days and 12 days has been widely employed in crop classification (Mestre-Quereda et al., 2020), crop monitoring (Nasirzadehdizaji et al., 2021) and soil moisture retrieval (Barbouchi et al., 2022).

Currently, coherence has been proven to serve as a useful indicator for crop monitoring (Villarroya-Carpio et al., 2022). By comparing temporal coherence of various crops with different phenological stages, a strong correlation has been observed between the dynamic behavior of coherence and the primary phenological periods of crops (Zhao et al., 2024). Recent researches have explored the relationship between Sentinel-1 coherence and vegetation indices. For example, utilizing normalized difference vegetation index (NDVI), dual polarimetric radar vegetation index (DpRVI), and other vegetation indices as foundational indicators for monitoring vegetation growth. Among them, a linear relationship has been established between coherence and vegetation indices for 18 different crops (Villarroya-Carpio and Lopez-Sanchez, 2023), and a mathematical relationship between NDVI and coherence was established as well (Cao et al., 2022). The quantitative assessment yielded a robust correlation between the temporal coherence and the vegetation indices across various crop growth seasons. Additionally, coherence plays a unique additional role in the field of crop classification. The synergistic use of coherence with backscattering coefficient significantly improves crop classification accuracy, indicating that the integration of interferometric coherence and polarimetric data constitutes a dependable information reservoir for crop monitoring and mapping purposes (Mestre-Quereda et al., 2020).

---

[*] Corresponding author.

However, the coherence usually obtained is based on the maximum likelihood estimator (Touzi et al., 1999), and the estimated uncertainty is particularly pronounced in vegetated areas with frequent growth changes, leading to overestimation (Villarroya-Carpio et al., 2022). Consequently, in addition to the limitations of the Sentinel-1 temporal baseline, obtaining accurate coherence for vegetation may be another challenge in crop monitoring and classification. Motivated by the above challenges, the primary objective of this study was to evaluate the effectiveness of unbiased coherence as a useful indicator for crop monitoring and classification, while conducting comparative analyses with biased coherence. To achieve this goal, spatiotemporal Sentinel-1 data covering the major growing cycles of economic crops in 2018 were obtained, with a revisit cycle of 12 days. Initially, we established the linear relationship between coherence and DpRVI, and analyzing the relationship between temporal coherence and crop growth and agricultural behavior. Subsequently, on the basis of consolidating the effectiveness of coherence in crop classification, we evaluated the advantages of unbiased coherence over biased coherence in crop classification, providing novel insights for refined crop classification.

The structure of the paper is as follows: Section 2 presents the study site and the acquired data. Then, Section 3 describes the preprocessing of coherence and the correction method for unbiased coherence, along with a brief overview of the random forest classification algorithm. A comparison of the results of unbiased coherence and biased coherence for crop monitoring and classification is presented in Section 4. Finally, Section 5 offers a summary and draws conclusions based on the findings of the study.

2. Study Materials

The study area lies within the representative agricultural area in London, Ontario, Canada (42°47'N to 42°55'N, 81°30'W to 81°40'W). Based on the local crop growth cycles, our study obtained 18 ascending Sentinel-1 datasets spanning from April 4, 2018, to October 25, 2018. These datasets comprise single look complex images in dual-polarization mode (VV and VH), with a total of 17 interferometric pairs of 12-day revisit cycle. Specifically, the temporal Sentinel-1 images covering our study area exhibit an incidence range of 30.3°-42.8° and a pixel spacing of 2.33m13.94m (range*azimuth). The precise location of the study area is depicted alongside the Sentinel-1 dual-polarization SAR image captured on May 10, 2018, as shown in Figure 1.

In 2018, the Geographic Information Technology and Applications (GITA) Laboratory at the University of Western Ontario (UWO) conducted monthly land cover surveys in the study area from April to October, and Figure 2 shows the ground truth data. The survey found that the crop types in the agricultural area were soybean, corn, winter wheat, alfalfa, grass, tobacco, and pumpkin. However, there were fewer fields for crops other than soybeans, corn, and winter wheat. Therefore, this study focuses on monitoring three primary economic crops, which are summer crops (soybean and corn) and winter crop (winter wheat). For summer crops, soybeans and corn have similar growth cycles, typically planted in May, matured in September, and harvested in October. In contrast, winter wheat, as a winter crop, is usually sown in October of the preceding year, matures in July, and is harvested from late July to early August of the following year. It is worth mentioning that the "others" category encompasses tobacco and pumpkin, and "forage" category consists of alfalfa and grass.
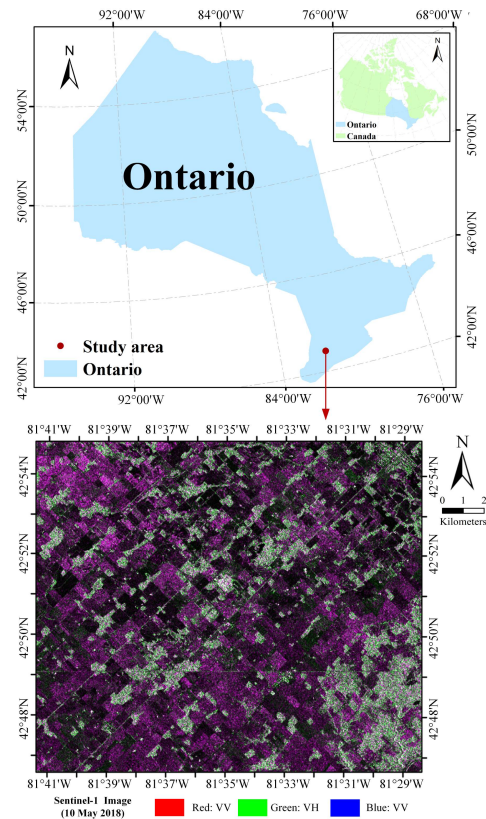

Figure 1. The location of study area and dual-pol Sentinel-1 image acquired on the 10/05/2018 (Red: VV, Green: VH, Blue: VV).
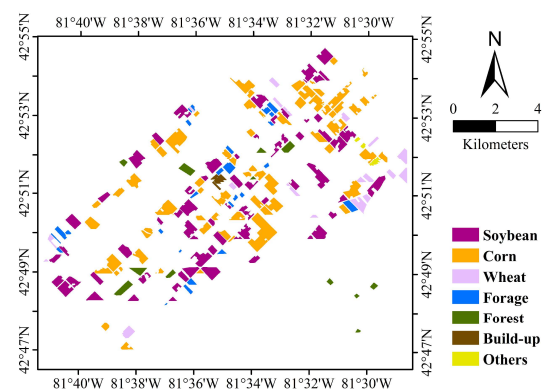

Figure 2. Ground truth data of the study area.

3. Methods

3.1 Preprocessing

The SNAP software serves as a toolbox for Sentinel data, with extensibility, portability, and a modular interface. In this study, preprocessing of Sentinel-1 images was carried out using the SNAP software (available online: http://step.esa.int/main/toolboxes/snap/, accessed on 27 Aug. 2022). The preprocessing involved seven steps to generate the coherence of two SAR images: (1) TopSAR split; (2) Orbit correcting; (3) Radiometric calibration; (4) Image coregistration; (5) Speckle filtering and coherence estimation using a window of 4×19 (azimuth× range); (6) Deburst; (7) Terrain correction. Furthermore, DpRVI feature

was obtained based on SNAP as well. This enabled a quantitative assessment of coherence effectiveness in crop monitoring by analyzing the correlation between coherence and DpRVI.

3.2 Coherence

Coherence, as a fundamental feature of interferometric SAR, can reflect the extent to which vegetation has changed between two acquisition date intervals. The coherence's obtained from the above preprocessing steps are based on the maximum likelihood method estimated over a moving window, which can be calculated with equation (1) (Touzi et al., 1999).

$$\gamma_{est} = \frac{\left|\sum_{n=1}^{N} S_1 S_2^*\right|}{\sqrt{\left(\sum_{n=1}^{N} S_1 S_1^*\right) \cdot \left(\sum_{n=1}^{N} S_2 S_2^*\right)}}, \quad (1)$$

where
S_1 and S_2 = the master and slave images
N = the number of samples of the moving window
| | = signify the absolute value operator
* = represents the complex conjugate

The window size for coherence estimation is directly proportional to the precision of coherence estimation. Despite utilizing a window size of 4*19 to minimize the bias, the coherence values show low levels due to the rapid changes in vegetation during the growing season (Jacob et al., 2020). In particular, especially in low coherence regions, the coherence estimates obtained by the maximum likelihood estimator tend to be higher. The bias compensation for coherence is given by (Touzi et al., 1999), is represented by the probability density function corresponding to moments of order k=1 in equation (2):

$$E(\gamma_{est}) = \frac{\Gamma(L)\Gamma(\frac{3}{2})}{\Gamma(L+1/2)} \cdot {}_3F_2\left(\frac{3}{2}, L, L; L+\frac{1}{2}, 1; \gamma^2\right) \cdot (1-\gamma^2)^L, \quad (2)$$

where
$_3F_2$ = the generalized hypergeometric function
L = the equivalent number of looks (ENL)

As indicated by equation (2), compensation for coherence bias requires the value of ENL. Here, ENL can be computed directly from the image by selecting a uniform region near the study area, typically from water bodies. equation (3) provides the method for calculating ENL using homogeneous regions from SAR intensity images:

$$ENL = \frac{\mu^2}{\sigma^2}, \quad (3)$$

where
μ = mean of homogeneous regions
σ^2 = variance of homogeneous regions

In this work, ENL values for a homogeneous region under 18 scenes of SLC images with dual polarization modes were obtained. When compensating for coherence bias, the interferometric pair with the lowest ENL values from the two scenes of SLC images was selected, which would avoid the problem of the region with low coherence value being zero after compensation as much as possible. Taking the VV polarization interferometric pair composed of June 15 and June 27 as an example, the relationship curve between the estimated coherence and the unbiased coherence can be obtained by using ENL = 41 with Eq. (2) (Figure 3). It is evident from Figure 3 that a bias exists in the estimated coherence, particularly when the coherence values are low. Consequently, the coherence corrected for bias is referred to as unbiased coherence, denoted by $\gamma_{unbiased}$, while the estimated coherence (γ_{est}), is referred to as biased coherence, denoted by γ_{biased}.
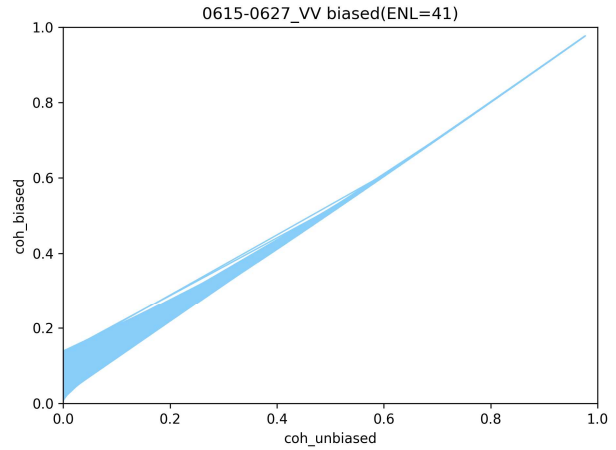

Figure 3. Coherence bias for the VV polarization interferometric pair 0615-0627 (with ENL=41).

3.3 Random Forest

The Random Forest classifier (RF) integrates the classification decisions of all decision trees, selecting the most frequent class as the final output (Breiman, 2001). By introducing randomness in sample and feature selection for each tree, RF effectively mitigates overfitting and demonstrates robustness against noise. These advantages make RF stand out in machine learning and widely used in crop classification (Liao et al., 2020; Xie et al., 2021). In this study, the random forest classifier has been implemented based on the scikit-learn toolkit of Python software, and the main settings classifier parameters are shown in Table 1.

Number	Hyperparameter	Value
1	Number of decision trees (n_estimators)	100
2	Minimum number of samples for the branch node (min_samples_split)	2
3	Minimum sample size of the leaves (min_samples_leaf)	1

Table 1. The information of tuning parameters for the RF classifier.

The input samples for the RF classifier are obtained by dividing the ground truth data into a training set and a test set based on the polygon level (field), since there is high correlation between neighboring pixels in the same field (Zhong et al., 2019). Specifically, the dataset was divided into five mutually exclusive subsets, each containing an equal number of pixels. Two subsets (40%) were selected as the testing set, while the remaining subsets (60%) formed the training set. In order to avoid any chance in classification, five repeated experiments were conducted, each employing different combinations of training and testing sets.

The RF employs the testing set to assess the accuracy of the classification. Our classification uses Overall Accuracy (OA), kappa coefficient, Producer's Accuracy (PA) and User's Accuracy (UA) as the metrics for accuracy evaluation, and calculates the standard deviation (STD) of each metric in multiple classification. It is worth mentioning that the above classification metrics are all derived from the confusion matrix.

4. Results

4.1 Crop Monitoring

To highlight the differences between biased and unbiased coherence more clearly, ground truth data were introduced to calculate the average coherence values of all known fields of the three crops (soybeans, corn, and winter wheat) at each date. This facilitated the construction of corresponding time series curves.
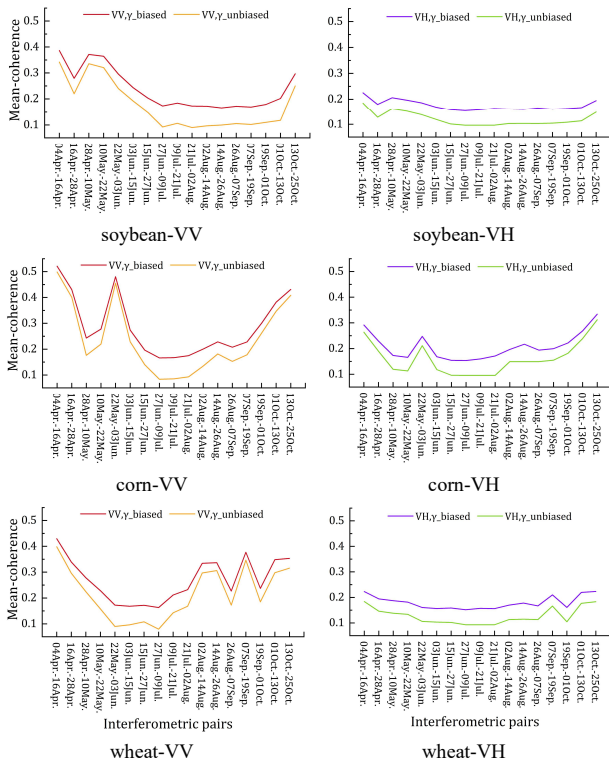

Figure 4. The temporal evolution of γ_{biased} and $\gamma_{unbiased}$ for major cash crops.

Figure 4 compares the time-series dynamics of the mean values of γ_{biased} and $\gamma_{unbiased}$ for the three crops throughout the growth cycle. Overall, there are similar temporal trends of unbiased coherence and biased coherence for both polarization channels (VV, VH), with $\gamma_{unbiased}$ consistently lower than γ_{biased}. This difference arises due to the significant temporal decorrelation caused by crop growth, resulting in decreased coherence values. Notably, γ_{biased} tends to overestimate in regions of low coherence, causing a loss of contrast and consequently leading to higher γ_{biased} values compared to the actual coherence.

It is noteworthy that there exists a correlation between coherence and crop phenology. This correlation is evident in the higher coherence values observed during the initial and harvesting stages of crop growth, while coherence values tend to decrease during the peak nutritional period of crop growth. However, there are significant differences in coherence values between VV and VH polarizations due to the phase difference, with VV coherence values being higher than VH coherence values. Besides, the temporal fluctuations in VV coherence are more pronounced, thus providing a better reflection of crop growth. This phenomenon can be attributed to the ability of co-pol (VV) to enhance volume scattering from vegetation and the dependence of the cross-pol (VH) in the C-band on the vegetation rather than

the ground, making VH more susceptible to temporal interference effects than VV (Manavalan, 2018).

Crop coherence time-series qualitatively reflect a correlation between coherence and crop growth. DpRVI plays a crucial role in time-series crop monitoring by accurately retrieving the biophysical parameters of crops through the effective integration of scattering wave information(Mandal et al., 2020). Hence, it is necessary to quantitatively evaluate the crop monitoring capability of coherence through linear correlation analysis with DpRVI. As illustrated in Figure 5, the time-series of DpRVI displays high values during early growth stages and harvest. This is similar to the behavior of time-series changes in coherence.
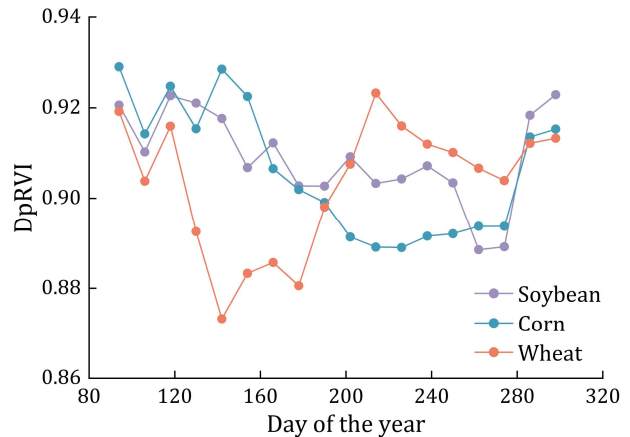

Figure 5. Time series of DpRVI for major cash crops.

Specifically, only 17 interference pairs (17 scene coherence) can be obtained from the 18 SAR images in this study, whereas DpRVI were available for all 18 dates. Therefore, the solution of linear interpolation is adopted to ensure the one-to-one correspondence between the two features. By analyzing the linear correlation between the coherence curves and DpRVI curves, the correlation coefficients (R) of three different crops under different polarizations were obtained, as presented in Table 2. This allowed for a quantitative assessment of the crop monitoring performance of both γ_{biased} and $\gamma_{unbiased}$.

	γ_{biased}		$\gamma_{unbiased}$	
Crop	**VV**	**VH**	**VV**	**VH**
Soybean	0.76	0.69	0.77	0.68
Corn	0.76	0.41	0.75	0.44
Wheat	0.75	0.49	0.76	0.43

Table 2. Coefficient of determination (R) for the linear regressions between coherence and DpRVI.

Upon analyzing the results in Table 2, it becomes evident that VV coherence exhibits a higher correlation with the vegetation index, consistent with the findings of coherence time series analysis. Among them, the difference between γ_{biased} and $\gamma_{unbiased}$ is small, which means that whether coherence has been corrected or not can monitor the vegetation growth effectively.

4.2 Crop Classification

In order to compare the contribution of γ_{biased} and $\gamma_{unbiased}$ to crop classification, two schemes of experiments were conducted, employing γ_{biased} and $\gamma_{unbiased}$ from different polarization channels as input features for the random forest classifier. It is noteworthy that to ensure comprehensive land cover

classification in the study area, seven land cover categories were taken into account in the classification. However, due to the small sample numbers of build-up and others, these two classes were excluded from the analysis of the results. Tables 3 and 4 show the classification results for obtained when using γ_{biased} and $\gamma_{unbiased}$ individually. In Tables 3 and 4, PA, UA, OA, and Kappa coefficients represent the average accuracy based on five classification experiments conducted with mutually exclusive training and testing sets. The symbol "±" indicates the standard deviation.

	$\gamma_{biased} - VV$		$\gamma_{biased} - VH$	
Class	**PA (%)**	**UA (%)**	**PA (%)**	**UA (%)**
Soybean	81.04±4.66	75.50±2.17	81.94±3.41	58.70±2.69
Corn	83.65±3.81	80.96±2.27	78.29±6.65	74.77±1.02
Wheat	62.69±12.10	80.83±6.40	2.77±0.70	36.16±12.01
Forage	15.26±2.17	31.59±9.41	0.14±0.09	11.37±5.56
Forest	76.57±3.78	67.76±5.03	3.42±0.64	31.46±4.29
	OA (%)	76.48±2.12	OA (%)	65.69±1.84
	Kappa	0.64±0.03	Kappa	0.43±0.03

Table 3. Classification accuracy using biased coherence based on different polarizations.

	$\gamma_{unbiased} - VV$		$\gamma_{unbiased} - VH$	
Class	**PA (%)**	**UA (%)**	**PA (%)**	**UA (%)**
Soybean	74.90±0.31	98.20±0.03	83.47±3.65	66.84±2.91
Corn	98.87±0.02	74.40±0.20	82.66±6.08	77.25±1.57
Wheat	73.76±0.43	98.14±0.16	24.53±3.41	88.14±7.21
Forage	74.33±0.42	98.21±0.30	32.38±1.50	98.88±0.61
Forest	73.27±0.72	97.91±0.22	34.48±1.03	95.30±1.11
	OA (%)	84.83±0.15	OA (%)	73.25±1.39
	Kappa	0.76±0.00	Kappa	0.57±0.02

Table 4. Classification accuracy using unbiased coherence based on different polarizations.

Overall, it is clear that unbiased coherence yields better classification results compared to biased coherence. The optimal classification scheme is based on the time-series feature set of $\gamma_{unbiased}$ in VV polarization, achieving an OA of 84.83% and a Kappa coefficient of 0.76. Across both polarization channels, $\gamma_{unbiased}$ consistently outperforms γ_{biased}, with an increase OA of 8.35% for VV and 7.56% for VH. These results underscore the ability of $\gamma_{unbiased}$ to provide more information about crops than γ_{biased}, thereby enhancing crop distinguishability. Moreover, VV coherence facilitates more precise crop classification, the overall accuracy of VV is more than 10% higher than that of VH. Additionally, the accuracy of each crop in VV polarization surpasses that in VH polarization, attributed to the lower signal-to-noise ratio in VH polarization.

When considering PA and UA of individual crops, soybean and corn have always shown good classification accuracy, with only slight improvements compared with $\gamma_{unbiased}$ and γ_{biased}. In contrast, the most significant enhancement attributed to $\gamma_{unbiased}$ features is observed for winter wheat, effectively reducing misclassification and omission errors present in γ_{biased}, resulting in PA and UA improvements of over 10%. Except for the three main cash crops, although the classification results among forage, forest and other crops are not ideal, the unbiased coherence can effectively distinguish them (UA > 95%). These findings underscore the valuable contribution of time-series unbiased coherence in crop classification.

5. Conclusions

In this study, we compared the abilities of biased and unbiased coherence in crop monitoring and classification. For this purpose, temporal coherence features of Sentinel-1 data were obtained, with the agricultural region in southwestern Ontario, Canada. The principal conclusions derived from the analysis conducted in this work can be summarized as follows:

(1) The VV coherence of the Sentinel-1 time series exhibits a strong correlation with DpRVI (R > 0.75), confirming VV coherence as the optimal indicator for assessing crop evolution. Among them, $\gamma_{unbiased}$ and γ_{biased} demonstrate similar trends and dynamic behavior, thereby sharing comparable levels of correlation with DpRVI. This suggests that the bias in coherence within vegetated areas has minimal impact on crop monitoring.

(2) Unbiased coherence outperforms biased coherence in crop classification, facilitating refined crop classification. Both polarizations show an OA increase of over 7.5% compared to γ_{biased}, leading to improved accuracy across all crop types. Notably, the temporal feature set ($\gamma_{unbiased}$) with VV polarization better reflects the differences between different crops, which yields the best classification results with an OA of 84.83% and a Kappa coefficient of 0.76.

In future studies, it is planned to consider more crop types and shorter temporal baselines to explore the additional role of unbiased coherence in crop growth monitoring and classification. Furthermore, bias compensation for coherence stands as a pivotal aspect in obtaining unbiased coherence, but low coherence values in certain regions may inevitably result in zero values after correction. Therefore, we aim to further investigate a more accurate method to obtain unbiased coherence, thereby mitigating the impact of zero coherence values. These will help to grasp the spatial and temporal changes of crop planting structure more clearly.

References

Barbouchi, M., Chaabani, C., Cheikh M'Hamed, H., Abdelfattah, R., Lhissou, R., Chokmani, K., Ben Aissa, N., Annabi, M., Bahri, H., 2022. Wheat Water Deficit Monitoring Using Synthetic Aperture Radar Backscattering Coefficient and Interferometric Coherence. *Agric.*, 12(7), 1032.

Bhogapurapu, N., Dey, S., Bhattacharya, A., Mandal, D., Lopez-Sanchez, J.M., McNairn, H., López-Martínez, C., Rao, Y.S., 2021. Dual-polarimetric descriptors from Sentinel-1 GRD SAR data for crop growth assessment. *ISPRS J. Photogramm. Remote Sens.*, 178, 20-35.

Breiman, L., 2001. Random forests. *Mach. Learn.*, 45, 5-32.

Cao, Y., Li, P., Hao, D., Lian, Y., Wang, Y., Zhao, S., 2022. Analysis of the Relationship between Vegetation and Radar Interferometric Coherence. *Sustainability,* 14(24), 16471.

Jacob, A.W., Vicente-Guijalba, F., Lopez-Martinez, C., Lopez-Sanchez, J.M., Litzinger, M., Kristen, H., Mestre-Quereda, A., Ziolkowski, D., Lavalle, M., Notarnicola, C., Suresh, G., Antropov, O., Ge, S., Praks, J., Ban, Y., Pottier, E., Mallorqui Franquet, J.J., Duro, J., Engdahl, M.E., 2020. Sentinel-1 InSAR Coherence for Land Cover Mapping: A Comparison of Multiple Feature-Based Classifiers. *IEEE J. Sel. Topics Appl. Earth Observ. Remote Sens.*, 13, 535-552.

Liao, C., Wang, J., Xie, Q., Baz, A.A., Huang, X., Shang, J., He, Y., 2020. Synergistic use of multi-temporal RADARSAT-2 and VENμS data for crop classification based on 1D convolutional neural network. *Remote Sens.*, 12, 832.

Manavalan, R., 2018. Review of synthetic aperture radar frequency, polarization, and incidence angle data for mapping the inundated regions. *J. Appl. Remote Sens.*, 12, 021501.

Mandal, D., Hosseini, M., McNairn, H., Kumar, V., Bhattacharya, A., Rao, Y.S., Mitchell, S., Robertson, L.D., Davidson, A., Dabrowska-Zielinska, K., 2019. An investigation of inversion methodologies to retrieve the leaf area index of corn from C-band SAR data. *Int. J. Appl. Earth Obs. Geoinf.*, 82, 101893.

Mandal, D., Kumar, V., Ratha, D., Dey, S., Bhattacharya, A., Lopez-Sanchez, J.M., McNairn, H., Rao, Y.S., 2020. Dual polarimetric radar vegetation index for crop growth monitoring using sentinel-1 SAR data. *Remote Sens. Environ.*, 247, 111954.

Mestre-Quereda, A., Lopez-Sanchez, J.M., Vicente-Guijalba, F., Jacob, A.W., Engdahl, M.E., 2020. Time-Series of Sentinel-1 Interferometric Coherence and Backscatter for Crop-Type Mapping. *IEEE J. Sel. Topics Appl. Earth Observ. Remote Sens.*, 13, 4070-4084.

Nasirzadehdizaji, R., Cakir, Z., Balik Sanli, F., Abdikan, S., Pepe, A., Calò, F., 2021. Sentinel-1 interferometric coherence and backscattering analysis for crop monitoring. *Comput. Electron. Agric.*, 185, 106118.

Rosen, P.A., Hensley, S., Joughin, I.R., Li, F.K., Madsen, S.N., Rodriguez, E., Goldstein, R.M., 2002. Synthetic aperture radar interferometry. *Proceedings of the IEEE*, 88, 333-382.

Touzi, R., Lopes, A., Bruniquel, J., Vachon, P.W., 1999. Coherence estimation for SAR imagery. *IEEE Trans. Geosci. Remote Sens.*, 37, 135-149.

Villarroya-Carpio, A., Lopez-Sanchez, J.M., 2023. Multi-Annual Evaluation of Time Series of Sentinel-1 Interferometric Coherence as a Tool for Crop Monitoring. *Sensors (Basel)*, 23(4), 1833.

Villarroya-Carpio, A., Lopez-Sanchez, J.M., Engdahl, M.E., 2022. Sentinel-1 interferometric coherence as a vegetation index for agriculture. *Remote Sens. Environ.*, 280, 113208.

Xie, Q., Lai, K., Wang, J., Lopez-Sanchez, J.M., Shang, J., Liao, C., Zhu, J., Fu, H., Peng, X., 2021. Crop monitoring and classification using polarimetric RADARSAT-2 time-series data across growing season: A case study in southwestern Ontario, Canada. *Remote Sens.*, 13, 1394.

Zhao, Q., Xie, Q., Peng, X., Lai, K., Wang, J., Fu, H., Zhu, J., Song, Y., 2024. Understanding the Temporal Dynamics of Coherence and Backscattering using Sentinel-1 Imagery for Crop-Type Mapping. *IEEE J. Sel. Topics Appl. Earth Observ. Remote Sens.*, 17, 6875-6893.

Zhong, L., Hu, L., Zhou, H., 2019. Deep learning based multi-temporal crop classification. *Remote Sens. Environ.*, 221, 430-443.